Synthesis and Coordination Chemistry of a Novel Bidentate Phosphine: 6-(Diphenylphosphino)-1,3,5-triaza-7-phosphaadamantane (PTA-PPh2)

Gene W. Wong, Jennifer L. Harkreader, Charles A. Mebi, and Brian J. Frost*

Department of Chemistry, University of Nevada, Reno, Nevada 89557

The upper rim of 1,3,5-triaza-7-phosphaadamantane (PTA) has been modified for the first time. Lithiation of PTA, with *n*-butyllithium, resulted in deprotonation of an α-phosphorus methylene and the formation of 1,3,5-triaza-7-phosphaadamantane-6-yllithium (PTA-Li). The chiral chelating phosphine 6-(diphenylphosphino)-1,3,5-triaza-7-phosphaadamantane (PTA-PPh2) was synthesized, in racemic form, by the reaction of PTA-Li with ClPPh2. PTA-PPh2 has been fully characterized in solution by multinuclear NMR spectroscopy and mass spectrometry and in the solid state by X-ray crystallography. The ^{31}P NMR spectrum contains a pair of doublets at −19.8 and −100.1 ppm (d, $^2J_{PP} = 65$ Hz). Unlike PTA, the new bidentate phosphine, PTA-PPh2, is insoluble in aqueous solutions. Two group 6 metal carbonyl complexes, [M(CO)4(PTA-PPh2)] (M = W and Mo), were synthesized by the addition of PTA-PPh2 to *cis*-[M(CO)4(pip)2] and characterized by NMR spectroscopy, IR spectroscopy, and X-ray crystallography. Also reported are the solid-state structures of *cis*-[W(CO)4PTA2], *cis*-[W(CO)4(PTA)(PPh3)], and [W(CO)4DPPM] (DPPM = diphenylphosphinomethane). PTA-PPh2 appears to be sterically similar to and slightly more electron-donating than DPPM.

Introduction

Progress in catalytic applications may often be correlated with either a steric or an electronic modification to the ligand set of the catalyst.[1] Indeed, small modifications can lead to large variation of the rate or product selectivity of a catalytic process. We have been interested in developing methods for the modification of 1,3,5-triaza-7-phosphaadamantane (PTA), first reported by Daigle et al.[2] in 1974 and introduced into aqueous phase catalysis by Joó, Darensbourg, and others.[3] Recently, there has been renewed interest in this neutral, water-soluble, and air-stable phosphine.[4,5] Thus far, modification of PTA has focused on alkylation of the phosphorus[6] or nitrogen[7] or modification of the "lower rim" of the ligand, i.e., the triazacyclohexane ring.[8−11]
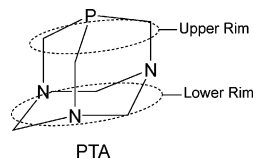
PTA — Upper Rim / Lower Rim

Figure 1 depicts an arrangement of PTA derivatives that have appeared in the literature including a ring-expanded
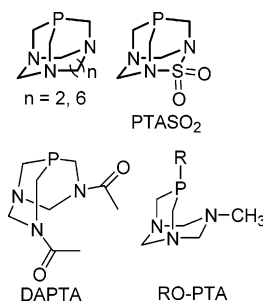
Figure 1. PTA derivatives. R = alkyl or aryl.

ligand,[8] PASO2,[9,10] DAPTA,[11] and a "ring-opened" PTA derivative (RO-PTA).[6] With the exception of the RO-PTA derivative, these PTA derivatives involve modification of the triazacyclohexane ring of PTA and are reasonably distant from phosphorus and therefore any coordinated metal center. Prior to the submission of this entry, there have been no reported modifications of the "upper rim" of PTA. Of interest is that substitution at the methylene adjacent to the phosphorus of PTA results in chiral phosphines, with the

* To whom correspondence should be addressed. E-mail: frost@chem.unr.edu.

(1) For example, see: (a) Van Leeuwen, P. W. N. M.; Kamer, P. C. J.; Reek, J. N. H.; Dierkes, P. *Chem. Rev.* **2000**, *100*, 2741−2770. (b) Van Leeuwen, P. W. N. M. *Homogeneous Catalysis: Understanding the Art*; Kluwer Academic Publishers: Dordrecht, The Netherlands, 2004.
(2) Daigle, D. J.; Pepperman, A. B., Jr.; Vail, S. L. *J. Heterocycl. Chem.* **1974**, *11*, 407−408.

stereogenic carbon in close proximity to the phosphorus and, therefore, any coordinated metal center. Herein we report the synthesis of 1,3,5-triaza-7-phosphaadamantane-6-yllithium (PTA-Li), which has allowed for the introduction of modifications to an α-phosphorus methylene of PTA. A new chiral bidentate phosphine based on PTA (PTA-PPh$_2$), as well as group 6 metal carbonyl derivatives of PTA-PPh$_2$, PTA, PPh$_3$, and DPPM, are reported.

Experimental Section

Materials and Methods. Unless otherwise noted, all manipulations were performed on a double-manifold Schlenk vacuum line under nitrogen or in a nitrogen-filled glovebox. Prior to use, solvents

(3) (a) Darensbourg, D. J.; Joó, F.; Kannisto, M.; Katho, A.; Reibenspies, J. H.; Daigle, D. J. *Inorg. Chem.* **1994**, *33*, 200−208. (b) Darensbourg, D. J.; Joó, F.; Kannisto, M.; Katho, A.; Reibenspies, J. H. *Organometallics* **1992**, *11*, 1990−1993. (c) Joó, F.; Nadasdi, L.; Benyei, A. Cs.; Darensbourg, D. J. *J. Organomet. Chem.* **1996**, *512*, 45−50. (d) Darensbourg, D. J.; Stafford, N. W.; Joó, F.; Reibenspies, J. H. *J. Organomet. Chem.* **1995**, *488*, 99−108. (e) Darensbourg, D. J.; Decuir, T. J.; Reibenspies, J. H. High Technology. In *Aqueous Organometallic Chemistry and Catalysis*; Horvath, I. T., Joo, F., Eds.; Kluwer: Dordrecht, The Netherlands, 1995; pp 61−80. (f) Laurenczy, G.; Joó, F.; Nadasdi, L. *Inorg. Chem.* **2000**, *39*, 5083−5088. (g) Kovacs, J.; Todd, T. D.; Reibenspies, J. H.; Joó, F.; Darensbourg, D. J. *Organometallics* **2000**, *19*, 3963−3969.
(4) For an excellent review of PTA chemistry, see: Phillips, A. D.; Gonsalvi, L.; Romerosa, A.; Vizza, F.; Peruzzini, M. *Coord. Chem. Rev.* **2004**, *248*, 955−993.
(5) (a) Frost, B. J.; Bautista, C. M.; Huang, R.; Shearer, J. *Inorg. Chem.* **2006**, *45*, 3481−3483. (b) Frost, B. J.; Miller, S. B.; Rove, K. O.; Pearson, D. M.; Korinek, J. D.; Harkreader, J. L.; Mebi, C. A.; Shearer, J. *Inorg. Chim. Acta* **2006**, *359*, 283−288. (c) Frost, B. J.; Mebi, C. A.; Gingrich, P. W. *Eur. J. Inorg. Chem.* **2006**, 1182−1189. (d) He, Z.; Tang, X.; Chen, Y.; He, Z. *Adv. Synth. Catal.* **2006**, *348*, 413−417. (e) Romerosa, A.; Campos-Malpartida, T.; Lidrissi, C.; Saoud, M.; Serrano-Ruiz, M.; Peruzzini, M.; Garrido-Cárdenas, J. A.; García-Maroto, F. *Inorg. Chem.* **2006**, *45*, 1289−1298. (f) Krogstad, D. A.; Cho, J.; DeBoer, A. J.; Klitzke, J. A.; Sanow, W. R.; Williams, H. A.; Halfen, J. A. *Inorg. Chim. Acta* **2006**, *359*, 136−148. (g) Lidrissi, C.; Romerosa, A.; Saoud, M.; Serrano-Ruiz, M.; Gonsalvi, L.; Peruzzini, M. *Angew. Chem., Int. Ed.* **2005**, *44*, 2568−2572. (h) Mebi, C. A.; Frost, B. J. *Organometallics* **2005**, *24*, 2339−2346. (i) Frost, B. J.; Mebi, C. A. *Organometallics* **2004**, *23*, 5317−5323. (j) Bolano, S.; Gonsalvi, L.; Zanobini, F.; Vizza, F.; Bertolasi, V.; Romerosa, A.; Peruzzini, M. *J. Mol. Catal. A* **2004**, *224*, 61−70. (k) Akbayeva, D. N.; Gonsalvi, L.; Oberhauser, W.; Peruzzini, M.; Vizza, F.; Brueggeller, P.; Romerosa, A.; Sava, G.; Bergamo, A. *Chem. Commun.* **2003**, 264−265.
(6) (a) Fluck, E.; Weissgraeber, H. J. *Chem.-Ztg.* **1977**, *101*, 304. (b) Assmann, B.; Angermaier, K.; Paul, M.; Riede, J.; Schmidbaur, H. *Chem. Ber.* **1995**, *128*, 891−900. (c) Assmann, B.; Angermaier, K.; Schmidbaur, H. *J. Chem. Soc., Chem. Commun.* **1994**, 941−942.
(7) (a) Daigle, D. J.; Pepperman, A. B. J. *J. Heterocycl. Chem.* **1975**, *12*, 579−80. (b) Forward, J. M.; Staples, R. J.; Fackler, J. P., Jr. *Z. Kristallogr.* **1996**, *211*, 129−130. (c) Forward, J. M.; Staples, R. J.; Fackler, J. P., Jr. *Z. Kristallogr.* **1996**, *211*, 131−132. (d) Forward, J. M.; Staples, R. J.; Liu, C. W.; Fackler, J. P., Jr. *Acta Crystallogr. C* **1997**, *53*, 195−197. (e) Pruchnik, F. P.; Smolenski, P. *Appl. Organomet. Chem.* **1999**, *13*, 829−836. (f) Pruchnik, F. P.; Smolenski, P.; Galdecka, E.; Galdecki, Z. *New J. Chem.* **1998**, *22*, 1395−1398. (g) Smolenski, P.; Pruchnik, F. P.; Ciunik, Z.; Lis, T. *Inorg. Chem.* **2003**, *42*, 3318−3322.
(8) (a) Navech, J.; Kraemer, R.; Majoral, J. P. *Tetrahedron Lett.* **1980**, *21*, 1449−1452. (b) Benhammou, M.; Kraemer, R.; Germa, H.; Majoral, J. P.; Navech, J. *Phosphorus Sulfur* **1982**, *14*, 105−119.
(9) (a) Daigle, D. J.; Boudreaux, G. J.; Vail, S. L. *J. Chem. Eng. Data* **1976**, *21*, 240−241. (b) Delerno, J. R.; Majeste, R. J.; Trefonas, L. M. *J. Heterocycl. Chem.* **1976**, *13*, 757−760. (c) Daigle, D. J.; Pepperman, A. B., Jr.; Boudreaux, G. *J. Heterocycl. Chem.* **1974**, *11*, 1085−1086.
(10) Darensbourg, D. J.; Yarbrough, J. C.; Lewis, S. J. *Organometallics* **2003**, *22*, 2050−2056.
(11) (a) Darensbourg, D. J.; Ortiz, C. G.; Kamplain, J. W. *Organometallics* **2004**, *23*, 1747−1754. (b) Siele, V. I. *J. Heterocycl. Chem.* **1977**, *14*, 337−339.

were distilled under nitrogen from the appropriate drying agent (sodium/benzophenone for tetrahydrofuran (THF) and hexanes; magnesium/iodine for methanol). Water was distilled and deoxygenated before use. Chlorodiphenylphosphine was distilled and stored at 5 °C under nitrogen. Anhydrous 1,2-dimethoxyethane (DME), *n*-butyllithium, diethyl ether, dichloromethane, piperidine (pip), bis(diphenylphosphino)methane (dppm), and deuterated NMR solvents were purchased from commercial sources and used as received. Tetrakis(hydroxymethyl)phosphonium chloride was obtained from Cytec and used without further purification. 1,3,5-Triaza-7-phosphaadamantane (PTA),[12] *cis*-[W(CO)$_4$(pip)$_2$],[13] *cis*-[Mo(CO)$_4$(pip)$_2$],[13] and *cis*-[W(CO)$_4$(PPh$_3$)$_2$][13] were synthesized as reported in the literature. All NMR spectra were recorded on either a Varian Unity Plus 500 FT-NMR spectrometer, a Varian NMR System 400, a GN 300 FT-NMR/Scorpio spectrometer, or a QE 300 FT-NMR/Aquarius spectrometer. ^{1}H and ^{13}C NMR spectra were referenced to a residual solvent relative to tetramethylsilane. Phosphorus chemical shifts are relative to an external reference of 85% H$_3$PO$_4$ in D$_2$O with positive values downfield of the reference. IR spectra were recorded on Perkin-Elmer 2000 FT-IR spectrometer, in a 0.1-mm CaF$_2$ cell for solutions or as a KBr pellet for solid samples. X-ray crystallographic data were collected at 100($\pm$1) K on a Bruker APEX CCD diffractometer with Mo Kα radiation (λ = 0.710 73 Å) and a detector-to-crystal distance of 4.94 cm. A full sphere of data were collected utilizing four sets of frames, 600 frames per set with 0.3° rotation about ω between frames, and an exposure time of 10 s/frame. Data integration, correction for Lorentz and polarization effects, and final cell refinement were performed using SAINTPLUS and corrected for absorption using SADABS or TWINABS. The structures were solved using direct methods followed by successive least-squares refinement on F^2 using the SHELXTL 5.12 software package.[14] Crystallographic data and data collection parameters are listed in Table 1.

Synthesis of 1,3,5-Triaza-7-phosphaadamantane-6-yllithium (PTA-Li). To a suspension of dried PTA (3.10 g, 19.7 mmol) in 40 mL of THF was slowly added at room temperature *n*-butyllithium (2.5 M, 11 mL, 27.5 mmol) over the course of 5 min. The reaction was stirred at room temperature until the evolution of butane was no longer observed (approximately 2.5−3 h). The suspension was filtered under nitrogen and the precipitate washed with hexanes (2 × 15 mL), resulting in 3.20 g of a fine white highly pyrophoric powder. A yield of >90% for the synthesis of PTA-Li was determined by quenching PTA-Li with D$_2$O and measuring the ratio of PTA-D/PTA by ^{31}P NMR spectroscopy.[15] PTA-D was characterized by ^{1}H, ^{13}C, and ^{31}P NMR spectroscopies. ^{1}H NMR (400 MHz, CDCl$_3$): 4.602 ppm (s, 6H, NC*H*$_2$N), 4.054 ppm (d, $^2J_{PH}$ = 10 Hz, 5H, PC*H*$_2$N, PC*HD*N). ^{13}C{^{1}H} NMR (100 MHz, CDCl$_3$): 73.66 ppm (vt, J_{PC} = 2 Hz, 3C, NC*H*$_2$N), 50.60 ppm (d, $^1J_{PC}$ = 20 Hz, 1C, PC*H*$_2$N), 50.575 ppm (d, $^1J_{PC}$ = 20 Hz, 1C, PC*H*$_2$N), 50.218 (vq, $^1J_{PC}$ = 21 Hz, $^1J_{DC}$ = 21 Hz, 1C, PC*HD*N). ^{31}P{^{1}H} NMR (162 MHz, CDCl$_3$): −102.52 ppm (s, PTA-D), −102.07 ppm (s, PTA).

Caution! PTA-Li is a highly pyrophoric solid, igniting violently upon exposure to air.

Synthesis of 6-(Diphenylphosphino)-1,3,5-triaza-7-phosphaadamantane (PTA-PPh$_2$; 1). PTA-Li (0.5240 g, 3.21 mmol) was suspended in 10 mL of anhydrous DME followed by the immediate addition of chlorodiphenylphosphine (2.23 mmol, 0.49 g) at room

(12) Daigle, D. J. *Inorg. Synth.* **1998**, *32* 40−3245.
(13) Darensbourg, D. J.; Kump, R. L. *Inorg. Chem.* **1978**, *17*, 2680−2682.
(14) *XRD Single-Crystal Software*; Bruker Analytical X-ray Systems: Madison, WI, 1999.
(15) See the Supporting Information for details.

Table 1. Summary of Data Collection, Solution, and Refinement Parameters for Compounds 1−4

	PTA-PPh$_2$ (1)	[W(CO)$_4$(PTA-PPh$_2$)] (2)	[Mo(CO)$_4$(PTA-PPh$_2$)] (3)	cis-[W(CO)$_4$(PTA)(PPh$_3$)] (4)
empirical formula	P(C$_6$H$_5$)$_2$C$_6$H$_{11}$N$_3$P	(CO)$_4$W(P(C$_6$H$_5$)$_2$C$_6$H$_{11}$N$_3$P)	(CO)$_4$Mo(P(C$_6$H$_5$)$_2$C$_6$H$_{11}$N$_3$P)	(CO)$_4$W(P(C$_6$H$_5$)$_3$)(PN$_3$C$_6$H$_{12}$)
fw	341.32	637.21	549.3	715.32
T (K)	100(2)	100(2)	100(2)	100(2)
wavelength (Å)	0.710 73	0.710 73	0.710 73	0.710 73
cryst syst	monoclinic	monoclinic	monoclinic	monoclinic
space group	$P2(1)/n$	$P2(1)/n$	$P2(1)/n$	$P2(1)/m$
a (Å)	14.357(2)	13.989(5)	14.005(7)	10.015(2)
b (Å)	6.2457(9)	11.657(4)	11.715(6)	12.534(3)
c (Å)	19.192(3)	14.086(5)	14.060(7)	11.605(2)
α (deg)	90	90	90	90
β (deg)	101.598 (3)	100.685(10)	101.200(10)	110.847(3)
γ (deg)	90	90	90	90
V (Å^3)	1685.8(4)	2257.1(14)	2262.9(2)	1361.4(5)
Z	4	4	4	2
D_{calcd} (Mg/m^3)	1.345	1.875	1.612	1.745
abs coeff (mm^{-1})	0.261	5.294	0.756	4.400
cryst size (mm^3)	0.12 × 0.05 × 0.03	0.15 × 0.11 × 0.05	0.66 × 0.29 × 0.10	0.14 × 0.08 × 0.03
θ range for data collection (deg)	1.62−26.00	1.88−30.00	1.88−32.27	1.88−32.37
index ranges	−17 ≤ h ≤ 17 −7 ≤ k ≤ 7 −23 ≤ l ≤ 23	−16 ≤ h ≤ 19 16 ≤ k ≤ 14 −19 ≤ l ≤ 19	−20 ≤ h ≤ 20 −17 ≤ k ≤ 17 −21 ≤ l ≤ 21	−15 ≤ h ≤ 13 −14 ≤ k ≤ 18 −17 ≤ l ≤ 17
reflns collected	18 907	17 503	39 784	14 622
independent reflns	3324 (R_{int} = 0.0683)	6490 (R_{int} = 0.0434)	7997 (R_{int} = 0.0207)	5022 (R_{int} = 0.0584)
abs correction	SADABS	SADABS	SADABS	SADABS
data/restraints/param	3324/0/208	6490/0/289	7997/0/373	5022/0/205
GOF on F^2	1.072	1.022	1.082	0.983
final R indices [$I > 2\sigma(I)$]	R1 = 0.0659, wR2 = 0.1791	R1 = 0.0376, wR2 = 0.0755	R1 = 0.0253, wR2 = 0.0723	R1 = 0.0387, wR2 = 0.0721
R indices (all data)	R1 = 0.0970, wR2 = 0.1949	R1 = 0.0565, wR2 = 0.0794	R1 = 0.0278, wR2 = 0.0738	R1 = 0.0540, wR2 = 0.0766
CCDC no.	603500	603501	603502	603503

temperature. The reaction was stirred overnight and DME removed under vacuum. The resulting yellow-white solid was washed with water to remove PTA and LiCl. The remaining solid was dissolved in a minimal amount of methanol/toluene (50:50, v/v) and purified by column chromatography (PTA-PPh$_2$; R_f value = 0.55), resulting in 75 mg of an off-white solid (0.22 mmol, 10% yield). ^{1}H NMR (400 MHz, CD$_2$Cl$_2$): 7.0−7.5 ppm (m, 10H, Ar), 5.25 ppm (dt, J = 2 and 14 Hz, 1H, P−CH−P), 3.6−4.8 ppm (m, 10H, NCH_2N, PCH_2N). ^{13}C{^{1}H} NMR (100 MHz, CD$_2$Cl$_2$): 135.4 ppm (dd, J_{PC} = 3 Hz, J_{PC} = 22 Hz, Ar), 132.9 ppm (d, J_{PC} = 18 Hz, Ar), 129.9 ppm (s, Ar), 128.7 ppm (m, Ar), 76.6 ppm (d, J_{PC} = 2 Hz, NCN), 74.5 ppm (s, NCN), 68.4 ppm (dd, $^3J_{PC}$ = 11 Hz, $^3J_{PC}$ = 2 Hz, N−C−N), 61.6 ppm (dd, $^1J_{PC}$ = 30 Hz, $^1J_{PC}$ = 14 Hz, 1C, P−CH−P), 52.2 (dd, J_{PC} = 23 Hz, J_{PC} = 4 Hz, PCN), 47.9 ppm (dd, J_{PC} = 23 Hz, J_{PC} = 3 Hz, PCN). ^{31}P{^{1}H} NMR (162 MHz, CD$_2$Cl$_2$): −19.8 ppm (d, $^2J_{PP}$ = 65 Hz, PPh$_2$), −100.1 ppm (d, $^2J_{PP}$ = 65 Hz, PTA). GC−MS (m/z): 342 (M$^+$) 156 (major fragment PN$_3$C$_6$H$_{11}$). Anal. Calcd for PTA-PPh$_2$: C, 63.34; H, 6.20; N, 12.31. Found: C, 63.07; H, 6.23; N, 12.15. X-ray-quality crystals were obtained by slow diffusion of diethyl ether into a methylene chloride solution of PTA-PPh$_2$, resulting in the formation of clear and colorless rods over the course of 1 week.

Synthesis of [W(CO)$_4$(PTA-PPh$_2$)] (2). PTA-PPh$_2$ was prepared from 0.48 g of PTA-Li (2.94 mmol) and chlorodiphenylphosphine (2.23 mmol, 0.49 g), as described above without purification by column chromatography. The addition of the crude PTA-PPh$_2$ to a degassed dichloromethane solution of cis-[W(CO)$_4$(NHC$_5$H$_{10}$)$_2$] (1.11 g, 2.38 mmol) under refluxing conditions afforded a yellow solution. The solution was filtered through Celite, and the volume was reduced under vacuum. The addition of methanol and cooling to 0 °C resulted in the isolation of 69 mg of 2 as a yellow crystalline

solid in 5% overall yield (44% based on a 10% yield of 1). ^{1}H NMR (400 MHz, CD$_2$Cl$_2$): 3.7−4.9 ppm (m, PCH_2N, NCH_2N, 10H), 5.63 (apparent triplet, $^2J_{PH}$ = 10 Hz, PCHP, 1H), 7.4−8.0 ppm (m, PPh$_2$, 10H). ^{13}C{^{1}H} NMR (100 MHz, CD$_2$Cl$_2$): 55.65 ppm (d, $^1J_{PC}$ = 10 Hz, PCH$_2$N), 56.20 ppm (d, $^1J_{PC}$ =17 Hz, PCH$_2$N), 69.26 ppm (d, $^3J_{PC}$ = 7 Hz, NCH$_2$N), 73.61 ppm (d, $^3J_{PC}$ = 6 Hz, NCH$_2$N), 77.35 ppm (t, $^3J_{PC}$ = 5 Hz, NCH$_2$N), 79.67 ppm (dd, $^1J_{PC}$ = 21 and 19 Hz, PCHP), 129−132 ppm (m, Ar), 135.33 (d, $^1J_{PC}$ = 15 Hz, Ar), 139.07 ppm (d, $^1J_{PC}$ = 15 Hz, 1C, PC_{ar}), 139.39 ppm (d, $^1J_{PC}$ = 15 Hz, 1C, PC_{ar}), 202.98 ppm (apparent triplet, $^2J_{PC}$ = 7 Hz, cis-CO), 203.77 ppm (apparent triplet, $^2J_{PC}$ = 7 Hz, cis-CO), 209.37 ppm (m, two trans-CO's). ^{31}P{^{1}H} NMR (162 MHz, CD$_2$Cl$_2$): 21.7 ppm (d, $^2J_{PP}$ = 26 Hz, $^1J_{PW}$ = 201 Hz, PPh$_2$), −89.5 ppm (d, $^2J_{PP}$ = 26 Hz, $^1J_{PW}$ = 185 Hz, PTA). IR ν_{CO} (CH$_2$Cl$_2$, cm^{-1}): 2017 (s), 1917 (sh), 1899 (s), 1881 (sh). Anal. Calcd for 2·2(CH$_2$Cl$_2$): C, 35.71; H, 3.12; N, 5.21. Found: C, 35.21; H, 3.19; N, 5.28. Crystals suitable for X-ray diffraction were obtained by slow diffusion of diethyl ether into a dichloromethane solution of 2, resulting in yellow blocks after a few days.

Synthesis of [Mo(CO)$_4$(PTA-PPh$_2$)] (3). The synthesis of 3 was accomplished in a manner analogous to that of 2. Crude PTA-PPh$_2$ (230 mg) and cis-[Mo(CO)$_4$(NHC$_5$H$_{10}$)$_2$] (240 mg, 0.63 mmol) were refluxed for 5 min in 20 mL of degassed dichloromethane. The reaction mixture was filtered through Celite and the volume reduced under vacuum to ~5 mL. The addition of methanol and cooling to 0 °C resulted in the precipitation of 38 mg (0.07 mmol) of crystalline 3; an 11% overall yield based on cis-[Mo(CO)$_4$(pip)$_2$]. ^{1}H NMR (500 MHz, CD$_2$Cl$_2$): 3.6−4.8 ppm (m, PCH_2N, NCH_2N, 10H), 5.60 ppm (apparent triplet, $^2J_{PH}$ = 10 Hz, PCHP, 1H), 7.4−8.0 ppm (m, PPh$_2$, 10H). ^{31}P{^{1}H} NMR (202 MHz, CD$_2$Cl$_2$): 37.3 ppm (d, $^2J_{PP}$ = 23 Hz, PPh$_2$), −64.9 ppm (d, $^2J_{PP}$ = 23 Hz, PTA).

**Scheme 1.** Synthesis of PTA-Li and Reaction with D$_2$O
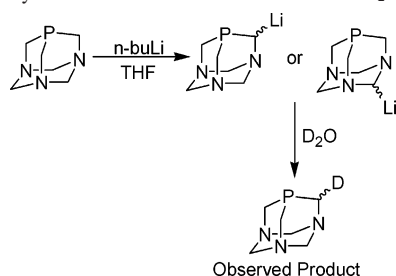
IR ν_{CO} (CH$_2$Cl$_2$, cm^{-1}): 2022 (m), 1923 (sh), 1908 (vs), 1889 (m). X-ray-quality crystals were obtained by layering a CH$_2$Cl$_2$ solution of **3** with diethyl ether, resulting in clear pale-yellow blocks.

Synthesis of cis-[W(CO)$_4$(PTA)(PPh$_3$)] (4). PTA (31 mg, 0.20 mmol) was added to a suspension of cis-[W(CO)$_4$(PPh$_3$)$_2$] (171 mg, 0.21 mmol) in dichloromethane. The reaction mixture was refluxed for 22 h and monitored periodically by ^{31}P NMR to obviate the formation of cis-[W(CO)$_4$(PTA)$_2$] (**5**). Upon cooling to room temperature, the solution was filtered through Celite and the solvent volume reduced to a minimum under vacuum. The product was isolated by column chromatography with toluene/methanol (4:1, v/v) as the eluant (R_f = 0.05 for **5**, 0.48 for cis-[W(CO)$_4$(PTA)-(PPh$_3$)], and 0.99 for cis-[W(CO)$_4$(PPh$_3$)$_2$]). Removal of the solvent under reduced pressure yielded 78 mg (0.11 mmol, 52% yield) of **4** as a pale-yellow powder. ^{1}H NMR (300 MHz, CD$_2$Cl$_2$): 7.48 ppm (m, 15H, C$_6$H$_5$), 4.34 ppm (AB q, 6H, PCH$_2$N), 3.75 ppm (s, 6H, NCH$_2$N). ^{31}P{^{1}H} NMR (121 MHz, CD$_2$Cl$_2$): 22.7 ppm (d, $^2J_{PP}$ = 21 Hz, $^1J_{PW}$ = 236 Hz, PPh$_3$), −80.3 ppm (d, $^2J_{PP}$ = 21 Hz, $^1J_{PW}$ = 218 Hz, PTA). IR ν_{CO} (CH$_2$Cl$_2$, cm^{-1}): 2017 (m), 1913 (sh), 1898 (vs), 1879 (sh). X-ray-quality crystals were obtained by the slow diffusion of diethyl ether into a dichloromethane solution of **4**, resulting in pale-yellow plates.

Results and Discussion

Synthesis of PTA-Li. The lithiation of PTA, yielding PTA-Li, was carried out in high yield by the addition of *n*-butyllithium to a suspension of PTA (Scheme 1). PTA-Li was isolated as an off-white highly pyrophoric powder in >90% yield. Because of its insolubility in common organic solvents and the extreme pyrophoric nature of PTA-Li, characterization was obtained based on the reaction of PTA-Li with D$_2$O. Reaction yields of PTA-Li were determined by integration of the PTA (−102.07 ppm) and PTA-D (−102.52 ppm) resonances obtained from the ^{31}P NMR spectrum of PTA-Li following reaction with D$_2$O.[15] Deuteration occurred regioselectively at an α-phosphorus methylene, as confirmed by ^{13}C NMR spectroscopy.[15] The ^{13}C NMR spectrum of PTA contains a single PCH$_2$N methylene resonance appearing as a doublet ($^1J_{CP}$ = 21 Hz) in CDCl$_3$. The PCH$_2$N region (approximately 50 ppm) of the ^{13}C NMR spectrum of PTA-D in CDCl$_3$ contains three sets of resonances: two doublets ($^1J_{PC}$ = 20 Hz) centered at 50.60 and 50.575 ppm resulting from the two inequivalent PCH$_2$N groups and an apparent quartet for the PCHDN group centered at 50.21 ppm. The apparent quartet arises from coupling of both the ^{31}P and ^{1}D nuclei to the ^{13}C nucleus with approximately the same coupling constant ($^1J_{CD} \sim {}^1J_{PC} \sim$ 21 Hz).

Synthesis and Characterization of PTA-PPh$_2$. The chiral bidentate phosphine PTA-PPh$_2$ was synthesized in low yield

Scheme 2. Synthesis of PTA-PPh$_2$
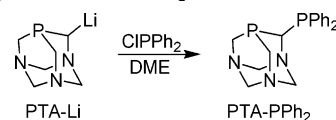
by the reaction of PTA-Li with chlorodiphenylphosphine in DME (Scheme 2). Other than PTA (resulting from protonation of PTA-Li), the major byproducts of the reaction were Ph$_2$P-PPh$_2$, Ph$_2$P(O)PPh$_2$, and Ph$_2$P(O)-(O)PPh$_2$, obtained from the reductive coupling of 2 equiv of ClPPh$_2$.[16] PTA-PPh$_2$ is no longer water-soluble, as a result of the addition of the large hydrophobic PPh$_2$ group to the PTA fragment, but is readily soluble in common organic solvents (e.g., CH$_2$Cl$_2$, CHCl$_3$, and CH$_3$OH). Protonation of PTA-PPh$_2$, presumably at a PTA nitrogen, in 1 M HCl(aq) results in a white solid that is insoluble in both water and common organic solutions. The ^{31}P{^{1}H} NMR spectrum of PTA-PPh$_2$ contains the expected pair of doublets at −19.8 and −100.1 ppm (d, $^2J_{PP}$ = 65 Hz), indicating two inequivalent phosphorus nuclei. The phenyl protons are observed as a multiplet between 7.0 and 7.5 ppm, integrating as 10 protons. The P−CH−P proton appears as a complex multiplet (apparent triplet of doublets) centered at 5.25 ppm, with the remaining PTA protons observed as a complex set of peaks between 3.6 and 4.8 ppm, integrating as 10 protons (PCH$_2$N and NCH$_2$N). The ^{13}C-{^{1}H} NMR spectrum contains two doublet of doublets at 47.9 and 52.2 ppm ($^1J_{PC}$ = 23 and 4 Hz) for the unmodified P−CH$_2$−N carbons of the PTA fragment and a doublet of doublets at 61.6 ppm ($^1J_{PC}$ = 30 and 14 Hz) for the carbon bound to both phosphorus nuclei. The N−C−N carbons appear in the region expected for PTA (73.5 ppm for PTA):[4,12] 68.4 (dd, $^3J_{PC}$ = 11 and 2 Hz), 74.5 (s), and 76.6 ppm (d, $^3J_{PC}$ = 2 Hz).

PTA is stable in air almost indefinitely; however, in CH$_2$Cl$_2$, PTA-PPh$_2$ is slowly oxidized preferentially at the PTA phosphorus. ^{31}P NMR spectra taken over time show that, concomitant with the loss of the doublet at −100.1 ppm, a doublet at −6.2 ppm ($^2J_{PP}$ = 40 Hz) grows in, which is close to the chemical shift observed for oxidized PTA, O=PTA (−2.5 ppm).[12] After 1 week, ~15% of PTA-PPh$_2$ was converted into O=PTA-PPh$_2$. The PPh$_2$ signal shifts slightly to −19.7 ppm ($^2J_{PP}$ = 40 Hz) upon oxidation of the PTA phosphorus. Oxidation of both phosphines of PTA-PPh$_2$ with H$_2$O$_2$ results in a ^{31}P NMR spectrum containing two doublets at −1.4 and 34.3 ppm ($^2J_{PP}$ = 4 Hz) for the O=PTA and O=PPh$_2$ phosphorus nuclei, respectively.

Structure of PTA-PPh$_2$. The solid-state structure of PTA-PPh$_2$ was determined by X-ray crystallography. Compound **1** crystallized in the centrosymmetric space group $P2(1)/c$, and both R and S enantiomers are present. A thermal ellipsoid representation of **1** is shown in Figure 2 along with selected bond lengths and angles. The P−C distances in **1** are perturbed relative to the parent PTA ligand (P−C$_{ave}$ = 1.856

(16) (a) Fluck, E.; Issleib, K. *Chem. Ber.* **1965**, *98*, 2674. (b) Russell, G. A.; Khanna, R. K. *Phosphorus Sulfur* **1987**, *29*, 271−274.
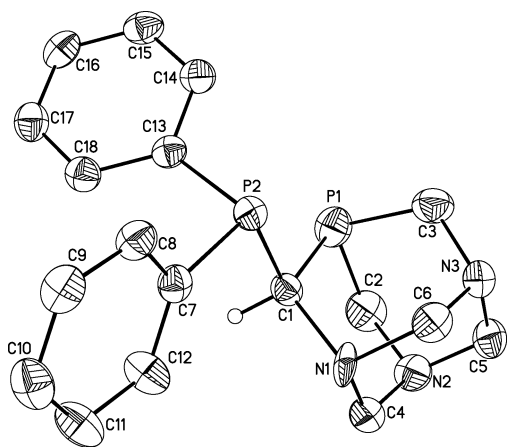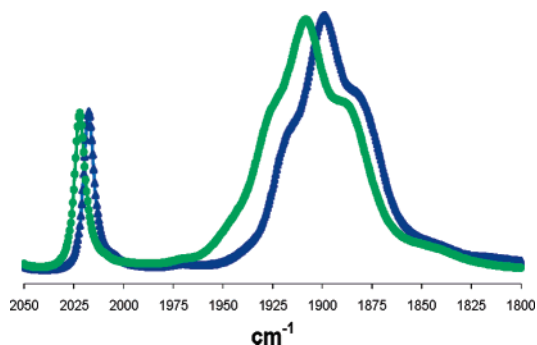
Figure 2. Representation of PTA-PPh₂ (**1**) along with the atomic numbering scheme (thermal ellipsoids are drawn at 50% probability). Only the *S* enantiomer is shown; however, both are present in the structure. Selected bond lengths (Å) and angles (deg): P1−C1 = 1.890(4); P1−C2 = 1.815(5); P1−C3 = 1.832(4); P2−C1 = 1.867(4); N1−C1 = 1.577(5); N1−C4 = 1.508(5); N1−C6 = 1.530(5); N2−C5 = 1.477(5); P1−C1−P2 = 108.79(18); P2−C1−N1 = 109.8(2).

Scheme 3. Synthesis of **2** and **3**
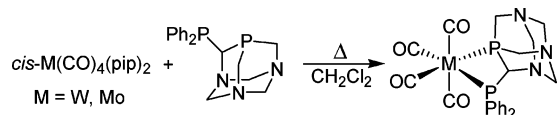
Å);[17] P1−C1 in **1** is elongated to 1.890(4) Å, and the P1−C2 and P1−C3 distances are slightly compressed to 1.815(5) and 1.832(4) Å, respectively. The P−C−P angle in PTA-PPh₂ of 108.79(18)° is comparable to the P−C−P angle observed in diphenylphosphinomethane (DPPM) of 106.2(3)°.[18]

Synthesis, Structure, and Spectral Properties of [M(CO)₄(PTA-PPh₂)] (M = W and Mo). The coordination chemistry of PTA-PPh₂ was explored through the synthesis of two group 6 metal carbonyl complexes by the addition of racemic PTA-PPh₂ to *cis*-[M(CO)₄Pip₂] (M = W and Mo) in refluxing CH₂Cl₂ (Scheme 3). The ³¹P NMR spectrum of **2** contained the expected pair of doublets centered at +21.7 (PPh₂) and −89.5 ppm (PTA), $^2J_{PP}$ = 26 Hz. Tungsten satellites were also observed, $^1J_{PTA-W}$ = 185 Hz and $^1J_{PPh_2-W}$ = 201 Hz. The molybdenum analogue, **3**, also displayed the expected pair of doublets in the ³¹P NMR spectrum centered at +37.3 (PPh₂) and −64.9 ppm (PTA), $^2J_{PP}$ = 23 Hz. These ³¹P NMR chemical shifts are consistent with other group 6 metal carbonyl complexes containing PTA: [Mo(CO)₅PTA], −55.9 ppm;[19] *cis*-[Mo(CO)₄PTA₂], −54.9 ppm;[19] [W(CO)₅-PTA], −78.4 ppm.[10,19] The carbonyl ligands trans to the phosphines appear in the ¹³C NMR spectrum of **2** as two apparent triplets at 202.98 ($^2J_{CP}$ = 7 Hz) and 203.77 ppm ($^2J_{CP}$ = 7 Hz). The two CO ligands cis to phosphorus appear as a complicated set of seven lines, centered at 209.37 ppm, resulting from the splitting of the chemically inequivalent

(17) (a) Jogun, K. H.; Stezowski, J. J.; Fluck, E.; Weidlein, J. *Phosphorus Sulfur* **1978**, *4*, 199−204. (b) Marsh, R. E.; Kapon, M.; Hu, S.; Herbstein, F. H. *Acta Crystallogr., Sect. B* **2002**, *B58*, 62−77.
(18) Schmidbaur, H.; Reber, G.; Schier, A.; Wagner, F. E.; Müller, G. *Inorg. Chim. Acta* **1988**, *147*, 143−150.
(19) Alyea, E. C.; Fisher, K. J.; Foo, S.; Philip, B. *Polyhedron* **1993**, *12*, 489−492.

Figure 3. IR spectra in the ν_{CO} region of **2** (▲) and **3** (●) in dichloromethane.

Table 2. IR ν_{CO} Stretching Frequencies of a Series of *cis*-[M(CO)₄L₂] Complexes [M = W and Mo; L₂ = (PTA)₂, (PPh₃)₂, PTA-PPh₂, DPPM]

	ν_{CO}, cm⁻¹			
complex[a]	A₁⁽²⁾	A₁⁽¹⁾	B₁	B₂
[W(CO)₄(PTA-PPh₂)] (**2**)	2018 (m)	1916 (sh)	1899 (vs)	1881 (sh)
[W(CO)₄(PPh₃)(PTA)] (**4**)	2017 (m)	1913 (sh)	1898 (vs)	1879 (sh)
[W(CO)₄(PTA)₂] (**5**)	2018 (m)	1917 (sh)	1900 (vs)	1883 (sh)
[W(CO)₄(PPh₃)₂]	2018 (m)	1939 (m)	1907 (sh)	1889 (vs)
[W(CO)₄(DPPM)] (**6**)	2018 (m)	1916 (sh)	1904 (vs)	1874 (m)
[Mo(CO)₄(PTA)₂][b,13]	2022 (m)	1930 (m)	1910 (sh)	1904 (sh)
[Mo(CO)₄(PPh₃)₂][b,13]	2023 (m)	1927 (m)	1908 (vs)	1897 (m)
[Mo(CO)₄(PTA-PPh₂)] (**3**)	2022 (m)	1923 (sh)	1908 (vs)	1889 (m)
[Mo(CO)₄(DPPM)][c,20]	2020 (m)	1920 (s)	1907 (vs)	1879 (vs)

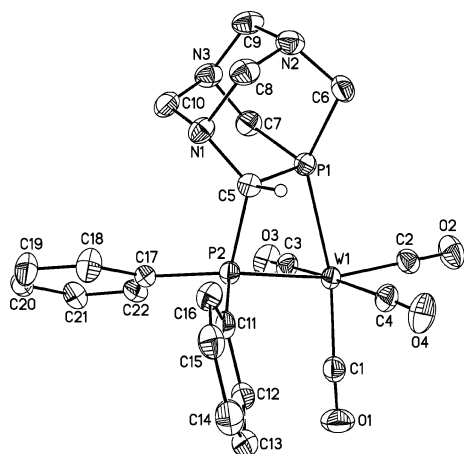[a] Spectra determined in CH₂Cl₂. [b] Solvent: tetrachloroethylene. [c] Solvent: ClCH₂CH₂Cl.

cis-CO ligands into doublet of doublets by the two phosphorus nuclei. IR spectra were obtained for both **2** and **3** with the expected pattern for complexes of pseudo C_{2v} symmetry (Figure 3); the molybdenum complex **3** appears at higher wavenumbers. Table 2 contains a comparison of the ν_{CO} region of the IR for a series of group 6 metal carbonyl complexes. On the basis of the IR data for the W(CO)₄L₂ series, PTA-PPh₂ is more electron-donating than (PPh₃)₂, slightly more electron-donating than DPPM, and comparable electronically to (PTA)₂ or a mixture of PTA and PPh₃.

The solid-state structures of **2** and **3** were determined by X-ray crystallography. Pale-yellow block crystals were obtained for both the tungsten and molybdenum analogues by layering a dichloromethane solution of **2** or **3** with diethyl ether. The two compounds are isostructural, with each containing a distorted octahedral metal center with four carbonyl ligands and the chelating PTA-PPh₂ ligand coordinated in a cis fashion as expected. Analogously, the solid-state structures of **1**−**3** crystallized in the centrosymmetric space group $P2_1/n$ and each structure contains both the *R* and *S* enantiomers of the chiral product. Thermal ellipsoid representations of **2** and **3** along with the atomic numbering scheme and selected bond lengths and angles may be found in Figures 4 and 5, respectively. In both compounds, the PTA phosphorus is slightly closer to the metal, P1−W1 = 2.4949(11) Å, P1−Mo1 = 2.5040(3) Å, relative to the PPh₂ phosphorus, P2−W1 = 2.5349(12) Å, P2−Mo1 = 2.5548-(3) Å. The carbonyl ligands trans to phosphorus (C1 and C2) have shorter M−C bonds than the mutually trans CO ligands (C3 and C4): W1−C1 = 1.986(5) Å, W1−C2 = 1.972(5) Å, W1−C3 = 2.037(5) Å, W1−C4 = 2.048(5) Å;

Figure 4. Thermal ellipsoid (50% probability) representation of **2** with the atomic numbering scheme. Only the *S* enantiomer is shown; however, both the *R* and *S* enantiomers are present in the structure. Selected bond lengths (Å) and angles (deg): W1−P1 = 2.4949(11); W1−P2 = 2.5349-(12); W1−C1 = 1.986(5); W1−C2 = 1.972(5); W1−C3 = 2.037(5); W1−C4 = 2.048(5); P1−C5 = 1.840(4); P2−C5 = 1.870(4); P1−W1−P2 = 68.18(4); P1−C5−P2 = 98.9(2); W1−P1−C5 = 94.21(13); W1−P2−C5 = 92.18(14); P1−W1−C1 = 169.02(14); P2−W1−C2 = 166.05(13); P1−W1−C2 = 98.51(13); P1−W1−C3 = 90.92(13); P2−W1−C1 = 101.24(14); P2−W1−C3 = 97.71(13); C3−W1−C4 = 174.14(17); C3−W1−C2 = 86.34(19).
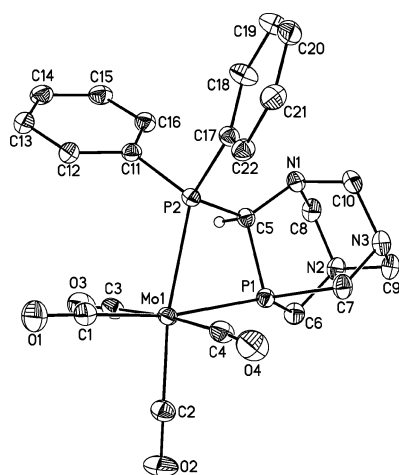
Figure 5. Thermal ellipsoid (50% probability) representation of **3** along with the atomic numbering scheme. Only the *R* enantiomer is shown; however, both the *R* and *S* enantiomers are present in the structure. Selected bond lengths (Å) and angles (deg): Mo1−P1 = 2.5040(3); Mo1−P2 = 2.5548(3); Mo1−C1 = 1.9881(13); Mo1−C2 = 1.9767(12); Mo1−C3 = 2.0490(13); Mo1−C4 = 2.0449(13); P1−C5 = 1.8449(11); P2−C5 = 1.8671(11); P1−Mo1−P2 = 68.370(10); P1−C5−P2 = 99.95(5); Mo1−P1−C5 = 93.72(3); Mo1−P2−C5 = 91.56(4); P1−Mo1−C1 = 169.42-(4); P2−Mo1−C2 = 166.71(4); P1−Mo1−C2 = 99.05(4); P1−Mo1−C3 = 93.98(4); P2−Mo1−C1 = 101.42(4); P2−Mo1−C3 = 87.10(4); C3−Mo1−C4 = 174.12(5); C2−Mo1−C3 = 89.62(5).

Mo1−C1 = 1.9881(13) Å, Mo1−C2 = 1.9767(12) Å, Mo1−C3 = 2.0490(13) Å, Mo1−C4 = 2.0449(13) Å. The bite angle, P1−M1−P2, is 68.18(4)° for **2** and 68.370(10)° for **3**, similar to the bite angle of the related dppm analogues at 67.108(16)° and 67.3(1)° for [W(CO)$_4$dppm] (vide infra) and [Mo(CO)$_4$-dppm],[21] respectively.

(20) Grim, S. O.; Briggs, W. L.; Barth, R. C.; Tolman, C. A.; Jesson, J. P. *Inorg. Chem.* **1974**, *13*, 1095−1100.

(21) Cheung, K. K.; Lai, T. F.; Mok, K. S. *J. Chem. Soc. A* **1971**, 1644−1647.

Table 3. ^{31}P NMR Chemical Shifts and Coupling Constants for **1** and a Series of *cis*-[W(CO)$_4$L$_2$] Complexes [L$_2$ = (PTA)$_2$, (PPh$_3$)$_2$, PTA-PPh$_2$, DPPM] in CD$_2$Cl$_2$

complex	^{31}P NMR	[2]J_{PP}, Hz	[1]J_{PTA-W}, Hz	[1]J_{PW}, Hz
PTA-PPh$_2$ (**1**)	−19.8, −100.1	65		
[W(CO)$_4$(PTA-PPh$_2$)] (**2**)	+21.7, −89.5	26	185	201
[W(CO)$_4$(PPh$_3$)(PTA)] (**4**)	+22.7, −80.3	21	218	236
[W(CO)$_4$(PTA)$_2$] (**5**)	−76.5			216
[W(CO)$_4$(PPh$_3$)$_2$]	+34.15			235
[W(CO)$_4$(DPPM)] (**6**)	−21.9			202

For comparison to complex **2**, we synthesized a series of related compounds by reaction of *cis*-[W(CO)$_4$(pip)$_2$] with PTA, PPh$_3$, and/or dppm: **4**, **5**, and [W(CO)$_4$(DPPM)] (**6**) (Tables 2 and 3). **4** was synthesized in modest yields through substitution of a triphenylphosphine ligand in *cis*-[W(CO)$_4$-(PPh$_3$)$_2$] by PTA. The ^{31}P NMR spectrum of the complex exhibits a pair of doublets at +22.7 and −80.3 ppm ([2]J_{PP} = 21 Hz) for the PPh$_3$ and PTA ligands, respectively, similar to the ^{31}P NMR spectrum of **2**. The [2]J_{PP} of 21 Hz is indicative of cis substitution.[22] Each phosphorus in the complex also couples to tungsten-183, giving rise to tungsten satellites, [1]J_{W-PTA} = 218 Hz and [1]J_{W-PPh_3} = 236 Hz. The W−P coupling constants in **4** are ~33 Hz larger than those observed for **2**, which are diminished because of the strain of the four-membered chelate ring in **3** relative to **4**.[20] The ^{31}P NMR resonance of the PTA ligand in **4** is shifted slightly upfield (−80.3 ppm) relative to that in **5** (−76.5 ppm) and may be due to steric strain, resulting in distortion of the octahedral geometry about the tungsten center as reported by Schenk and Buchner.[22] The ^{31}P NMR resonance resulting from the PPh$_3$ ligand at 22.7 ppm correlates well with that observed for other *cis*-[W(CO)(PPh$_3$)(PR$_3$)] complexes (e.g., 22.9 ppm for *cis*-[W(CO)$_4$(PPh$_3$)P(OPh)$_3$]).[22] The tungsten phosphorus couplings, [1]J_{PW}, observed for *cis*-[W(CO)$_4$-(PPh$_3$)$_2$] and *cis*-[W(CO)$_4$(PPh$_3$)(PTA)] are significantly larger than the corresponding [1]J_{PW} couplings observed in **2** (Table 3). This is at least partially due to distortion of the tungsten center from an ideal octahedron, although this likely does not account for the entire difference. IR spectra for compounds **2**−**6** (Table 2) reveal that these compounds have similar electronic environments. PTA-PPh$_2$ is more electron-donating than PPh$_3$ and DPPM and similar electronically to PTA or a mixture of PTA and PPh$_3$.

The solid-state structure of **4** was determined by X-ray crystallography (Table 1). Crystals were obtained by slow diffusion of diethyl ether into a CH$_2$Cl$_2$ solution of **4**, resulting in pale-yellow plates. Figure 6 contains the thermal ellipsoid representation and atomic numbering scheme of **4**. The tungsten center is in a distorted octahedral environment with P1−W1−P2 = 100.60(4)°, C1−W1−P1 = 171.36(15)°, C3−W1−P2 = 88.28(10)°, and C3−W1−C3A = 165.8(2)°. The W−P distances in **4**, W1−P1 = 2.5043(13) Å and W1−P2 = 2.5151(13) Å, are consistent with other tungsten carbonyl phosphine structures. Interestingly, the W−P1 distance in **4** is slightly longer than that for [W(CO)$_4$PTA-

(22) Schenk, W. A.; Buchner, W. *Inorg. Chim. Acta* **1983**, *70*, 189−196.

(23) Bernal, I.; Reisner, G. M.; Dobson, G. R.; Dobson, C. B. *Inorg. Chim. Acta* **1986**, *121*, 199−206.
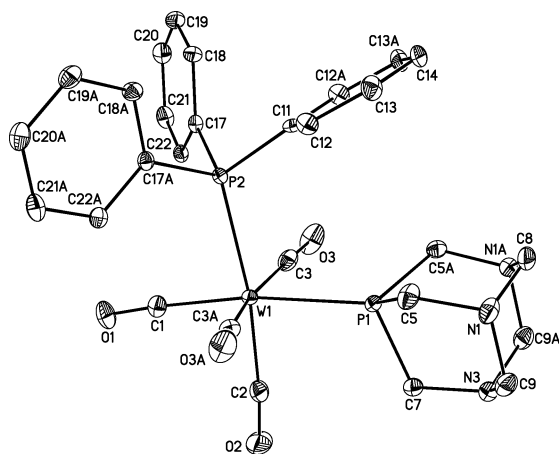
Figure 6. Thermal ellipsoid (50% probability) representation of **4** along with the atomic numbering scheme. Selected bond lengths (Å) and angles (deg): W1−P1 = 2.5043(13); W1−P2 = 2.5151(13); W1−C1 = 1.995(5); W1−C2 = 2.009(5); W1−C3 = 2.026(4); P1−C5 = 1.844(4); P2−C11 = 1.823(5); P1−W1−P2 = 100.60(4); P1−W1−C1 = 171.36(15); P1−W1−C2 = 87.57(15); P1−W1−C3 = 83.53(10); P2−W1−C1 = 88.04(15); P2−W1−C3 = 88.28(10); C3−W1−C3A = 165.8(2); C3−W1−C2 = 92.68(10).

Table 4. Comparison of Selected Bond Lengths (Å) and Angles (deg) for *cis*-[M(CO)₄L₂] (M = Mo and W; L = Phosphine Ligand)
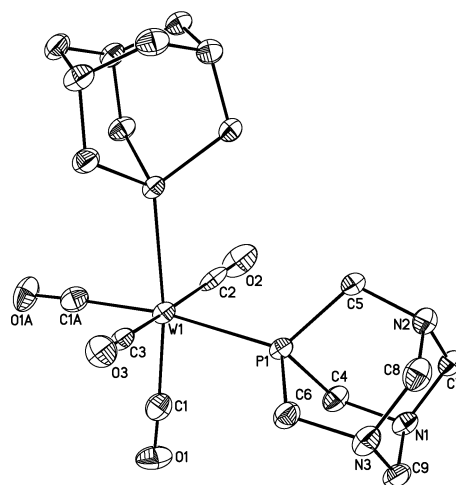
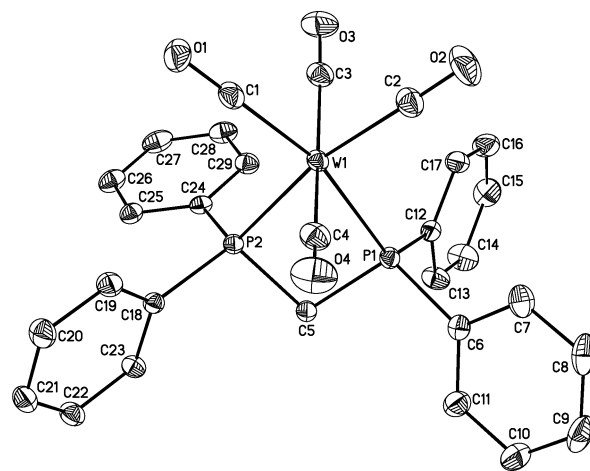|	bond lengths (Å)		bond angle (deg)
compound	M1−P1	M1−P2	P1−M1−P2
[W(CO)₄(PTA-PPh₂)] (**2**)	2.4949(11)	2.5349(12)	68.18(4)
[W(CO)₄(PTA)(PPh₃)] (**4**)	2.5043(13)	2.5151(13)	100.60(4)
[W(CO)₄(PTA)₂] (**5**)	2.4804(10)	2.4804(10)[a]	100.66(5)
[W(CO)₄(dppm)] (**6**)	2.5291(5)	2.5070(5)	67.108(16)
[Mo(CO)₄(PTA-PPh₂)] (**3**)	2.5040(3)	2.5548(3)	68.370(10)
[Mo(CO)₄(dppm)][21,20]	2.535(3)	2.501(2)	67.3(1)
[Mo(CO)₄(dppe)][23]	2.500(2)	2.495(2)	80.2(1)

[a] Generated by symmetry.

PPh₂], and the W1−P2 distance in **4** is slightly shorter than the corresponding distance in [W(CO)₄PTA-PPh₂] (Table 4). The solid-state structures of the previously reported complexes [W(CO)₄DPPM][20] and *cis*-[W(CO)₄PTA₂][19] were also determined by X-ray crystallography. Figures 7 and 8 contain thermal ellipsoid representations of **5** and **6**, respectively, along with the atomic numbering scheme and selected bond lengths and angles. Table 4 contains structural comparisons of compounds **2−6**.

Conclusion

We have reported here the results of lithiation of PTA leading to PTA-Li. Utilizing this reactive synthon, we synthesized a new chiral chelating phosphine, PTA-PPh₂, based on the PTA framework. The racemic form of PTA-PPh₂ was fully characterized in both solution and the solid state; unfortunately, this ligand does not carry all of the desirable properties of PTA, namely, water solubility. However, the ability to modify PTA, through lithiation, at an α-phosphorus methylene opens up a great deal of possibilities in the development of new phosphine ligands with the potential to be water-soluble. Of particular interest is that PTA compounds modified in this manner lead to chiral phosphine ligands, in which the stereogenic center is adjacent to phosphorus and therefore in close proximity to a coordinated metal. We are currently developing methodologies to

Figure 7. Representation of **5** with the atomic numbering scheme (thermal ellipsoids are drawn at 50% probability). Selected bond lengths (Å) and angles (deg): W1−P1 = 2.4804(10); W1−C1 = 2.003(5); W1−C2 = 2.011(8); W1−C3 = 2.046(7); P1−C5 = 1.841(4); P1−W1−P1A = 100.66(5); P1−W1−C1 = 87.69(13); P1−W1−C1A = 171.65(13); P1−W1−C2 = 89.09(15); P1−W1−C3 = 83.62(11); C1−W1−C2 = 91.1(2); C2−W1−C3 = 168.5(3); C1−W1−C3 = 97.45(18).

Figure 8. Thermal ellipsoid representation of **6** with the atomic numbering scheme (thermal ellipsoids are drawn at 50% probability). Selected bond lengths (Å) and angles (deg): W1−P1 = 2.5291(5); W1−P2 = 2.5070(5); W1−C1 = 1.980(2); W1−C2 = 1.993(2); W1−C3 = 2.029(2); W1−C4 = 2.036(2); P1−C5 = 1.8532(19); P2−C5 = 1.8523(19); P1−W1−P2 = 67.108(16); P1−C5−P2 = 97.39(9); P1−W1−C1 = 164.76(6); P2−W1−C2 = 167.64(6); P1−W1−C2 = 100.54(6); P1−W1−C3 = 98.31(6); P2−W1−C1 = 97.84(6); P2−W1−C3 = 95.22(6); C3−W1−C4 = 167.96(8); C3−W1−C2 = 85.97(9).

circumvent the low yields obtained for the PTA derivatives, presumably, due to the bulky nature of the PTA-Li nucleophile.

Supporting Information Available: Synthesis of PTA-D, *cis*-[W(CO)$_4$PTA$_2$], and [W(CO)$_4$DPPM]; NMR spectra of PTA-D, PTA-PPh$_2$, O=PTA-P(O)Ph$_2$, and **2**; IR spectra of compounds **4**−**6**; crystallographic details for **5** and **6**; full bond lengths and angles; and CIF files for compounds **1**−**6**. This material is available free of charge via the Internet at http://pubs.acs.org.